Solder Joint Reliability of Middle P% and High P% Ni/Au with Low Melting Point Solder Containing Indium

Mutsumi Komeyama, Toma Sasaki, Fuminori Shibayama, Katsuhisa Tanabe, Shigeo Hashimoto
C. Uyemura & Co., Ltd.
Osaka, Japan

ABSTRACT

In the early 2000s, the use of lead (Pb) was banned due to environmental and human health concerns and Pb-free solder alloys have been developed. Sn-Ag-Cu (SAC solder) is the most popular Pb-free solder alloy, but it has a high melting point above 217°C. Recently, as applications become more diverse, low-temperature soldering (LTS) alloys such as Sn-Bi and Sn-In have been required for various advantages. Since solder joint reliability (SJR) is closely related to the type of surface finish (SF), it is necessary to select an appropriate SF and then control the composition of intermetallic compounds (IMC) for LTS with good SJR.

In this study, the SJR between electroless Ni-P/immersion Au (ENIG) and low-melting-point solder containing indium was evaluated by ball grid array (BGA) substrates and high-speed shear tests (HSS). The results showed that the shear strength of ENIG with middle phosphorus content electroless Ni-P (MP-Ni) decreased after multiple reflows. On the other hand, the ENIG with high phosphorus content electroless Ni-P (HP-Ni) had a good LTS reliability and it was maintained even after multiple reflows. The IMC observation revealed that ENIG with HP-Ni did not have excessive IMC growth, while ENIG with MP-Ni formed thicker IMC after multiple reflows. Moreover, the composition of IMC and its existence ratio at the solder joint interface also greatly varied depending on the P% of the electroless Ni-P. In particular, the IMC which was identified as InP was the key factor for the difference of LTS reliability between ENIG with MP-Ni and ENIG with HP-Ni. The role of InP and the mechanism of IMC formation were clarified by various analyses. In conclusion, it was suggested that a higher P% of electroless Ni-P might be advantageous in LTS on the ENIG when using low-melting-point solder containing indium.

Key words: Low-temperature soldering (LTS), ENIG, P% in Ni-P deposit, Indium

INTRODUCTION

Sn-Bi and Sn-In are well known as typical low-melting-point solders. However, the adoption of these solder materials has been limited due to the brittleness caused by the segregation of bismuth (Bi), the high cost of indium (In) and their lack of strength. Many studies in recent years have focused on improving the mechanical performance of Sn-Bi and Sn-In solder alloys, for example by adding a third metal [1,2]. When using new solder materials, it is important to select an appropriate SF for it, because the SF has a key role to maintain good SJR by controlling the IMC composition and volume. There have been several studies regarding the combination of low-melting-point solder and SF, mostly with Sn-Bi solder alloys [3,4,5]. Nowadays many materials suppliers have developed low-melting-point solders, and Sn-In based alloys are also available as well as Sn-Bi based alloys. However, there was not much research for the combination of low-melting-point solder containing indium and SF. There are still many unknowns regarding the optimal SF and each layer's thickness, the composition of the formed IMCs, the mechanism of IMC formation, and so on.

The ENIG consists of electroless Ni-P/immersion Au and is the SF that is commonly and widely known. Electroless Ni serves as a diffusion barrier for Cu base metal, while Au provides good solderability and oxidation resistance. This study focuses on the difference in SJR between ENIG with MP-Ni and ENIG with HP-Ni using low-melting-point solder containing indium and clarifies the mechanism that causes the difference through IMC analysis by Field Emission Scanning Electron Microscope (FE-SEM), Energy Dispersive X-Ray Spectroscopy (EDS), and Transmission Electron Microscope (TEM) analyses.

EXPERIMENTAL METHOD

For HSS tests to evaluate the SJR, copper-plated substrates which were coated with solder mask and imaged to form 0.5 mm diameter pads were used. Substrates were plated using ENIG with MP-Ni (P = 7 wt%) and ENIG with HP-Ni (P = 11 wt%) utilizing plating chemicals commercially available from C. Uyemura & Co., Ltd.. Table 1 shows the plating process. The thicknesses of each deposit were measured by X-ray fluorescence coating thickness gauge (FT-150; Hitachi).

Table 1: Plating processes of the ENIG

Process	ENIG with MP-Ni	ENIG with HP-Ni
Cleaner	O	O
Soft etching	O	O
Acid rinse	O	O
Pd activator	O	O
Electroless Ni-P (P = 7 wt%)	O (6.0 - 7.0 μm)	– – –
Electroless Ni-P (P = 11 wt%)	– – –	O (6.0 - 7.0 μm)
Electoroless Au for MP-Ni	O (0.05 mm)	- - -
Electoroless Au for HP-Ni	- - -	O (0.05 μm)

The low-melting-point solder paste used is a commercially available mixture of a low-melting-point alloy containing indium and a SAC alloy (Durafuse LT with Indium10.8HF flux, type 4; Indium Corporation). It was printed on the plated pads manually with a dispenser (ML-6000X-GP; Musashi Engineering, Inc.) as shown in Figure 1. The reflow profile shown in Figure 2 was applied for making solder balls. The amount of applied paste was adjusted to make a 0.6 mm diameter solder balls after reflow. SJR was measured by HSS test (4000 HS; Nordson DAGE) as shown in Table 2.

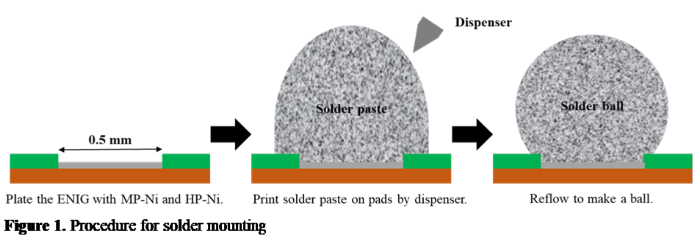

Figure 1: Procedure for solder mounting

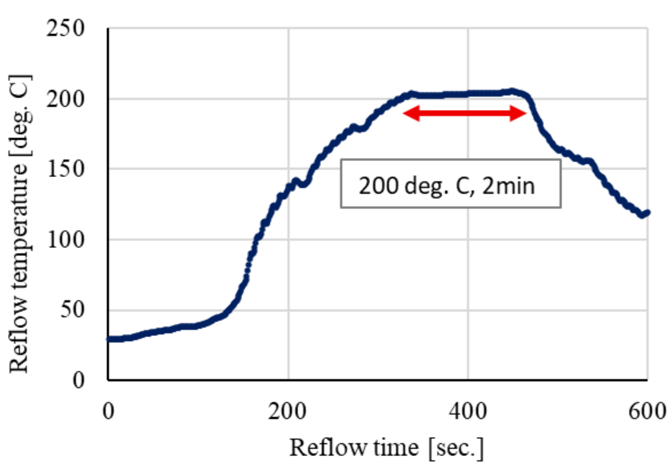

Figure 2: Reflow profile (ramp rate: 1-2 deg. C/sec, peak temperature and hold time: 2 min at 200-210 deg. C, cooling rate: 0.5-6 deg. C/sec)

Table 2: High speed shear test conditions

High speed shear test conditions	
Reflow equipment	UNI-6116α / ANTOM
Reflow envirionment	Air
Solder paste	A mixture of a low-melting-point alloy containing indium and a SAC alloy
Flux	Contained in solder paste
Deflux	After one time reflow
Solder diameter	about 0.60 mm
Pad diameter	0.50 mm
Reflow condition	200 deg. C, 2 min
The number of reflow	1 - 10 times
High speed shear test equipment	Dage 4000 HS
Shear speed	2000 mm/s
Tool height	10 μm

The cross-sectional images of IMC after mounting the solder ball were observed by FE-SEM (Ultra55 / Carl Zeiss) with EDS (Octane plus / EDAX) after polishing by cross-sectional polisher (CP) (SM-09010 / JEOL) or cooling CP (IB-19520CCP / JEOL) using liquid nitrogen.

TEM samples were prepared by the focused ion beam (XVISION210DB / Hitachi High-Technology) and were measured by STEM and EDS as shown in Table 3.

Table 3: TEM conditions

TEM and EDS conditions	
Equipment	JEM-F200 / JEOL
Acceleration voltage	200 kV
EDS	JED-2300T

RESULTS AND DISCUSSION

Solder joint reliability by HSS test

The SJR was evaluated using the HSS test, which was evaluated by the shear strength (maximum strength) and energy (integration of the shear strength and displacement: blue area in Figure 3). Solder paste was printed and mounted at maximum 200 deg. C, 2 min as shown in Figure 2. Reflows from 1 to 10 times were performed to clarify the difference between ENIG with MP-Ni and ENIG with HP-Ni. The shear strength and energy were evaluated based on the average of testing 20 solder balls.

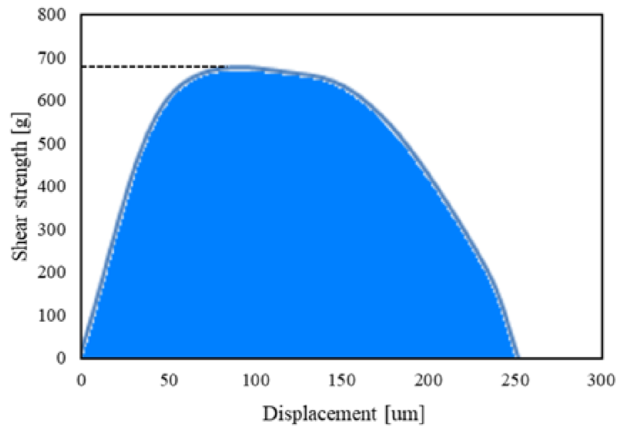

Figure 3: The shear strength and energy of HSS test

Figure 4 shows the results of the HSS test. In this study, all fractures occurred at the IMC interface. The shear strength and energy showed similar trends overall. The shear strength and energy after 1 time reflow were not different between ENIG with MP-Ni and ENIG with HP-Ni. However, these values of ENIG with MP-Ni decreased dramatically as the number of reflows increased and subsequently these were kept at low values. On the other hand, in ENIG with HP-Ni, the shear strength and energy gradually decreased as the number of reflows increased, so these values after 5 times reflow were higher than those of ENIG with MP-Ni . The changes between 1 time and 5 times reflow are important since it is recommended no more than three times reflow in the industry.

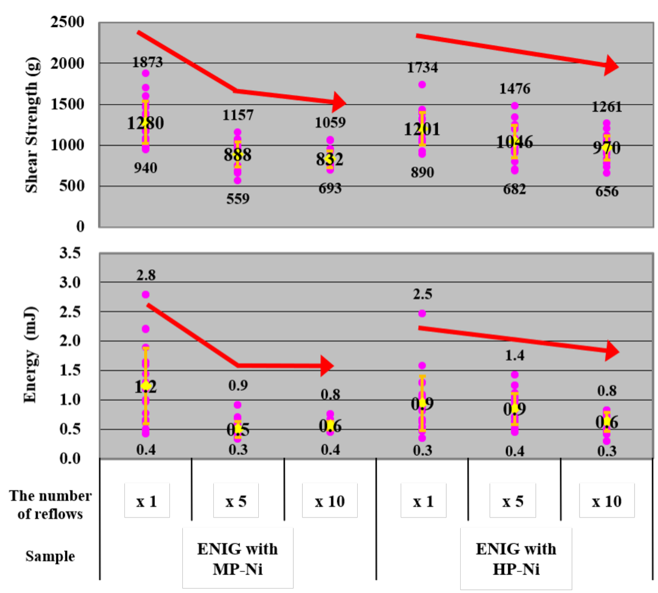

Figure 4: HSS test results of ENIG with MP-Ni and ENIG with HP-Ni after 1, 5 and 10 times reflow. (yellow markers: average value with standard deviation)

Cross-sectional view

A cross-sectional observation was conducted to confirm the IMCs at the interface between the plating layer and solder and to investigate the causes of differences in shear strength and energy. In the case of ENIG with MP-Ni, the IMC layer grew thicker with the number of reflows as shown in Figure 5. At the beginning of solder jointing, (Ni,Cu)3Sn4 was abundant, but as the number of reflows increased, the proportion of needle-shaped IMC, (Ni,Cu)3(In,Sn)7, increased. The block-shaped IMC, (Cu,Ni)6Sn5, was always present in small amounts regardless of the number of reflows. In addition, there were many small voids in the P-rich layer and the IMC layer. In contrast, the IMC layer in ENIG with HP-Ni was thinner than that of ENIG with MP-Ni as shown in Figure 6. There were also small voids, but they were clustered together in the upper part of the P-rich layer. As shown in Figure 6-2, the location and number of small voids were totally different between ENIG with MP-Ni and ENIG with HP-Ni.

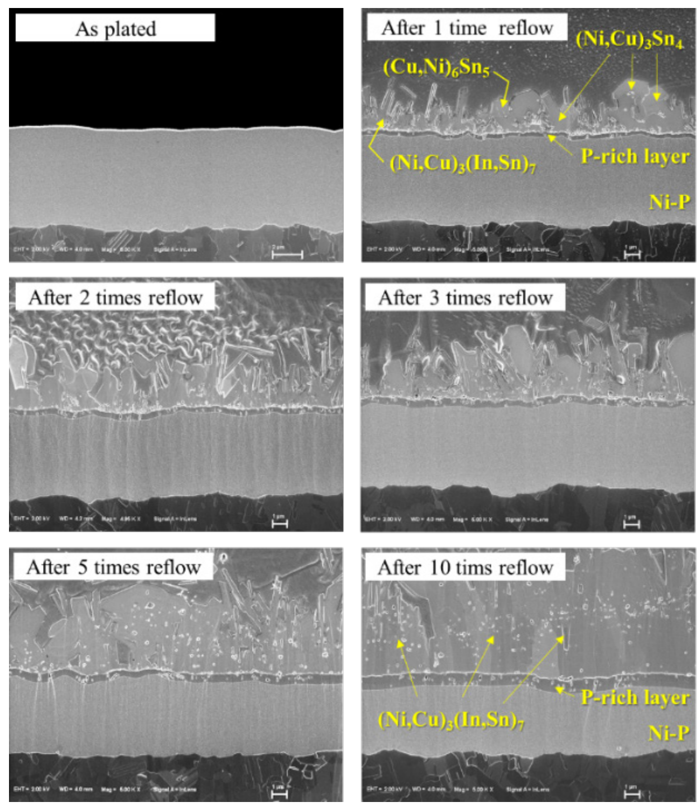

Figure 5: Cross-sectional SEM images of ENIG with MP-Ni as plated and after 1, 2, 3, 5 and 10 times reflow. (x5,000)

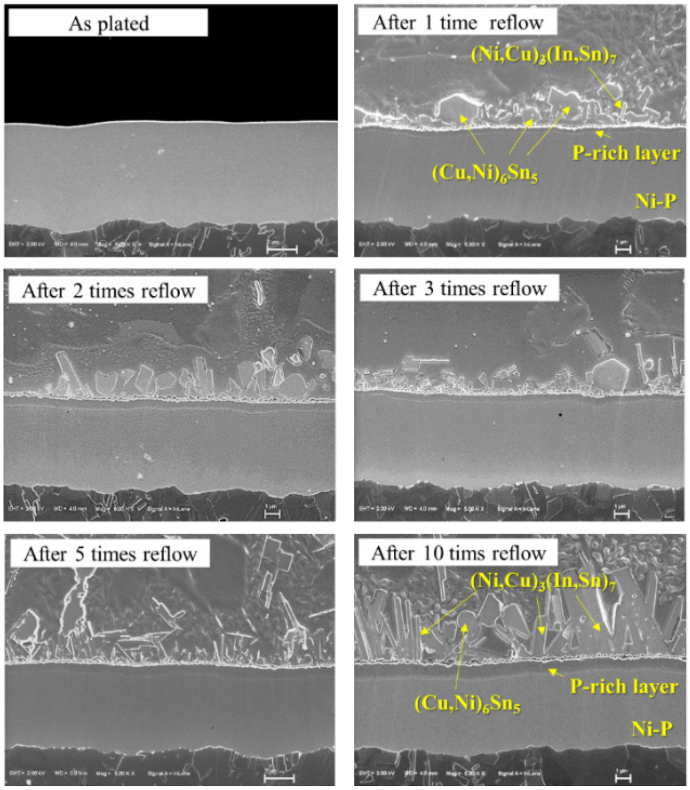

Figure 6: Cross-sectional SEM images of ENIG with HP-Ni as plated and after 1, 2, 3, 5 and 10 times reflow. (x5,000)

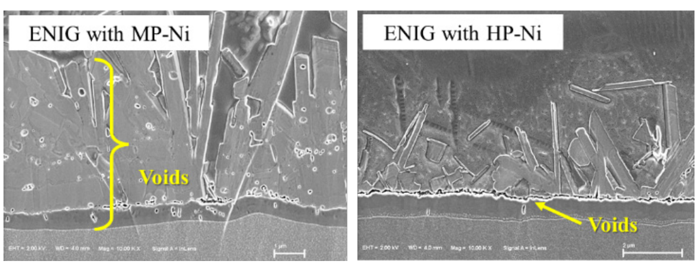

Figure 6-2: Cross-sectional SEM images of ENIG with MP-Ni and ENIG with HP-Ni after 5 times reflow. (x10,000)

It was suspected that the observed small voids might have been caused by damage during CP, so the sample preparation method was changed as shown in Figure 7. Originally, the first CP was performed at -120 deg. C using liquid nitrogen, then the second CP was processed at room temperature for an additional 10 sec. before observation to make the IMC shape easier to see. It was attempted to skip the second CP step because there was a possibility that low-melting-point solder and its IMC could be damaged by it. Substrates after 1, 5, and 10 times reflow were processed by the modified method. The cross-sectional observation revealed that there were no voids but "black IMCs" were observed as shown in Figure 8 and 9. In addition, there was dark colored "Increased P-rich area" where the P% was 2~3% higher than in other parts of the P-rich layer.

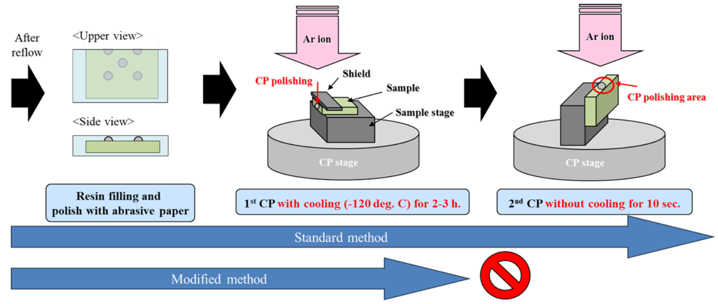

Figure 7: Sample preparation methods.

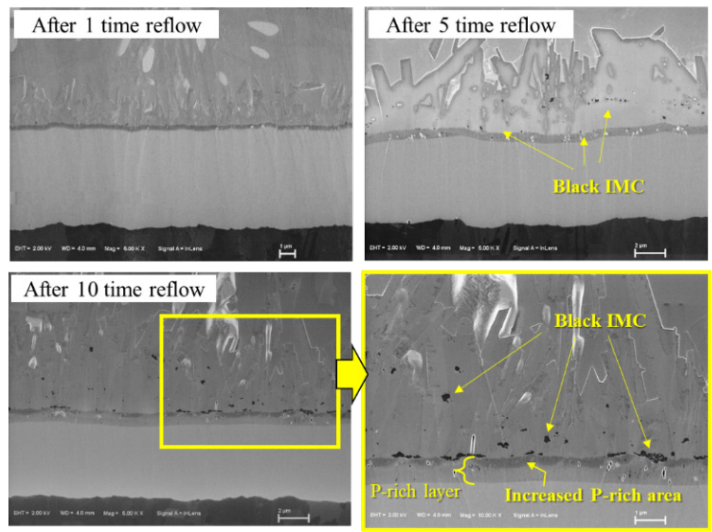

Figure 8: Cross-sectional SEM images of ENIG with MP-Ni prepared by modified method after 1, 5, 10 times reflow. (x5,000 and x10,000: the yellow-framed figure)

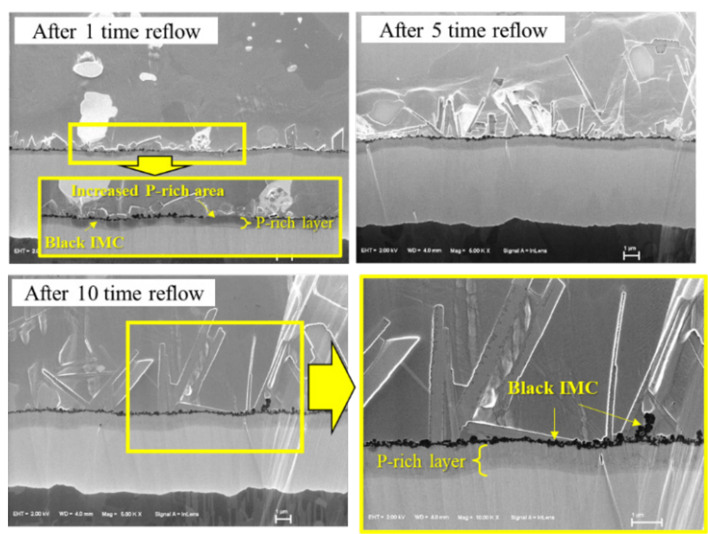

Figure 9: Cross-sectional SEM images of ENIG with HP-Ni prepared by modified method after 1, 5, 10 times reflow. (x5,000 and x10,000: the yellow-framed figure)

The location of the newly observed black IMC and the thickness of increased P-rich areas differed between ENIG with MP-Ni and ENIG with HP-Ni. In the case of ENIG with MP-Ni, the black IMCs diffused into the solder and the IMC layer, and increased P-rich areas were only observed after 10 times reflow. On the other hand, in ENIG with HP-Ni, the black IMC was formed as a uniform layer above the P-rich layer and did not diffuse into the solder and the IMC layer. Therefore, this black IMC layer may have the function to inhibit the growth of other IMCs, P-rich layer and increased P-rich area in ENIG with HP-Ni. The black IMC was too thin to identify the composition by EDS point analysis. However, EDS elemental maps showed strong indium and phosphorus peaks, while other elements spectrums were not detected at all as shown in Figure 10 and 11.

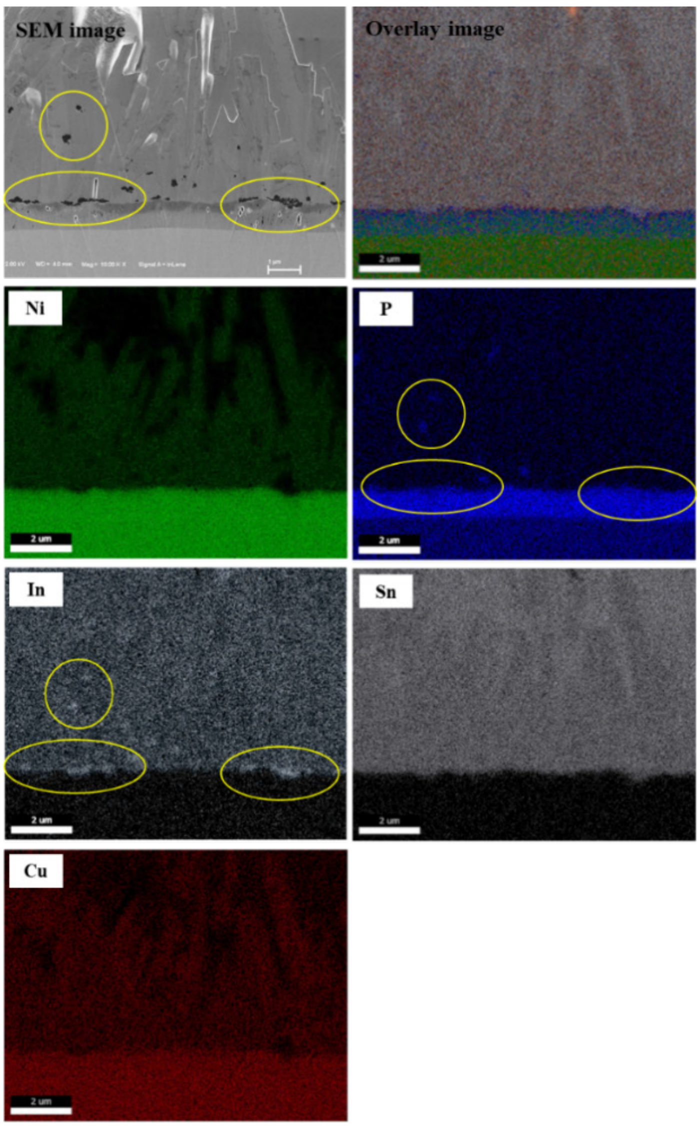

Figure 10: EDS elemental maps of ENIG with MP-Ni after 10 times reflow. (x5000)

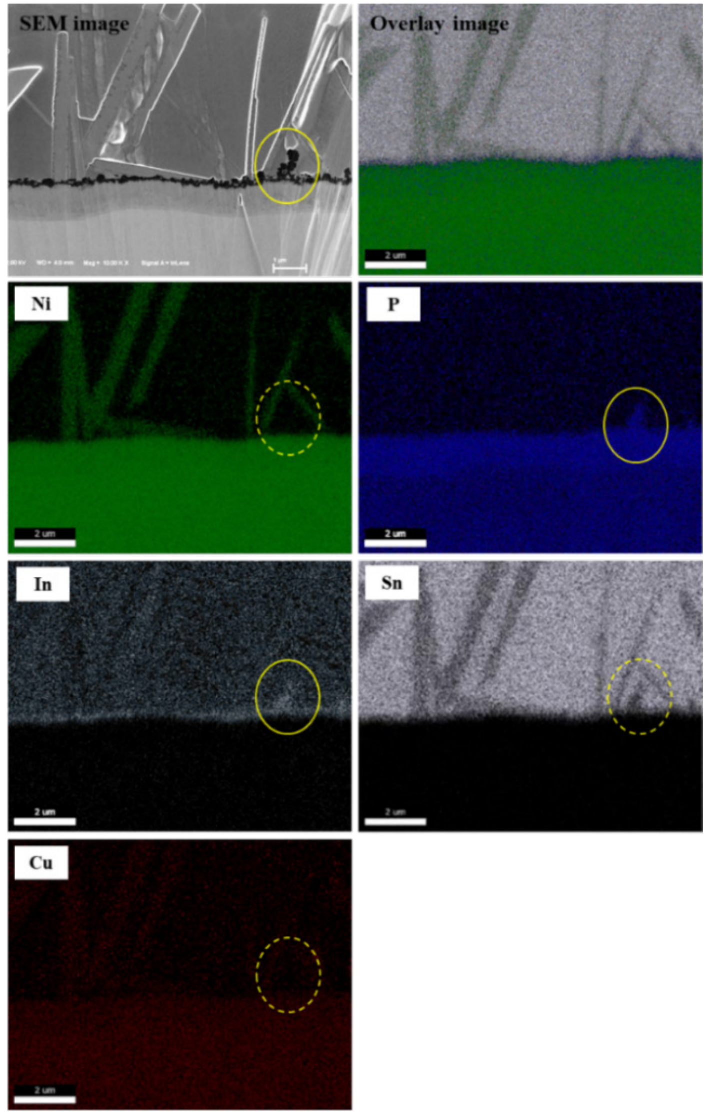

Figure 11: EDS elemental maps of ENIG with HP-Ni after 10 times reflow. (x5000)

STEM and EDS analysis

To investigate the black IMC in more detail, STEM and EDS analyses were performed in ENIG with HP-Ni after 10 times reflow as shown in Figure 12 and 13. EDS elemental maps confirmed strong detection of indium and phosphorus in the black IMC layer. Point analysis detected 59.3 at% of indium and 40.7 at% of phosphorus as shown in Figure 13(a), suggesting that the black IMC is InP. Figure 14(b) is the selected area diffraction pattern (SADP) of the black IMC. This appears to similar to one of the InP crystal structures, a zinc blende (ZB) structure [6], but further investigation is necessary because it is unclear.

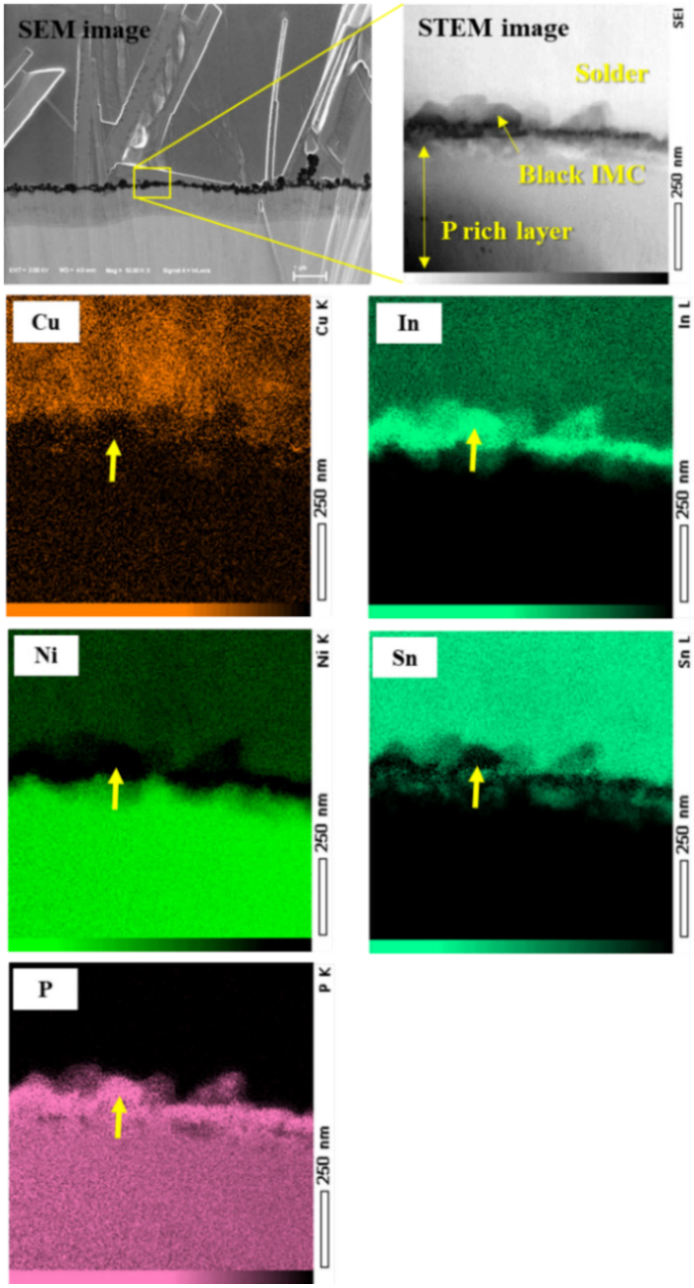

Figure 12: Cross-sectional dark field STEM image and EDS elemental maps of ENIG with HP-Ni after 10 times reflow.

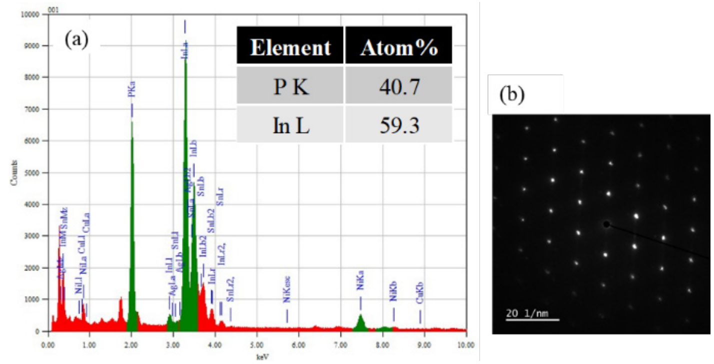

Figure 13: (a) EDS spectrum and quantitative analysis and (b) SADP of black IMC in ENIG with HP-Ni after 10 times reflow.

Discussion of the IMC formation mechanism and its relationship with SJR

Figure 14 illustrates the schematic diagram of the IMC forming mechanism. In ENIG with MP-Ni, (Ni,Cu)3Sn4 is the major IMC initially. Phosphorus is concentrated slowly, and the reaction interface of IMC forming is covered by (Ni,Cu)3Sn4, so there is little opportunity for indium and phosphorus to react. After that, (Ni,Cu)3Sn4 changes to (Ni,Cu)3(In,Sn)7 and phosphorus is more concentrated by IMC growth. IMC containing indium encounters "increased P-rich area", and then InP is formed and diffuses into the solder with IMC growth. The shear strength decreases rapidly due to IMC thickening or an increase in the amount of (Ni,Cu)3(In,Sn)7. On the other hand, HP-Ni causes rapid IMC formation and phosphorus is concentrated, so that InP layer is formed after 1 time reflow in ENIG with HP-Ni. It is considered that the uniform InP layer suppresses the other IMCs formation speeds and the amount of total IMC after multiple reflows is much smaller than that of ENIG with MP-Ni. The amount of (Cu,Ni)3(In,Sn)7 on the interface gradually increased and the shear strength decreases little by little.

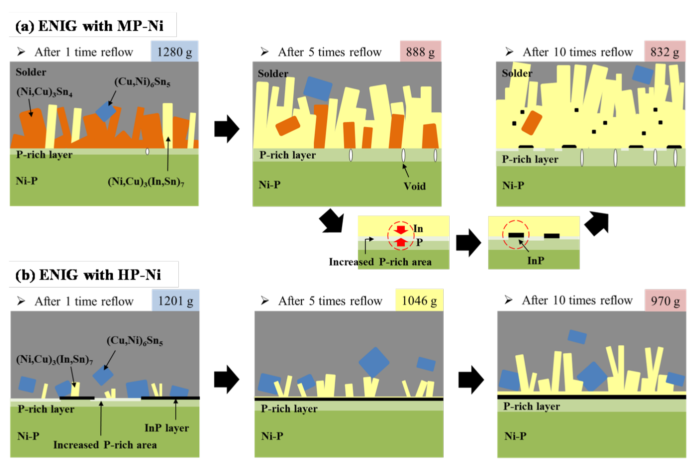

Figure 14: Schematic diagram of the IMC formation mechanism in ENIG with MP-Ni (a) and ENIG with HP-Ni (b).

CONCLUSIONS

This study evaluated the SJR between ENIG and low-melting-point solder containing indium and investigated how the P% of Ni-P deposit affects it. The shear strength and energy significantly decreased in ENIG with MP-Ni after multiple reflows, but not as much in ENIG with HP-Ni. In ENIG with HP-Ni, the IMC layer was thinner than that of ENIG with MP-Ni. The biggest difference between the IMCs of ENIG with MP-Ni and ENIG with HP-Ni was the formed location of the black IMC, which is composed of indium and phosphorus and assumed to be InP. Regarding ENIG with HP-Ni, the uniform InP layer suppressed the other IMCs formation speed. As a result, the IMC was thinner, and the shear strength and energy did not decrease as much as in ENIG with MP-Ni after multiple reflows. In conclusion, when using low-melting-point solder containing indium, ENIG with HP-Ni is considered to be more advantageous than ENIG with MP-Ni for LTS. This will be a useful suggestion for selecting the optimal SF for LTS.

REFERENCES

[1] Morgana Ribas, Ph.D., Divya Kosuri, Raghu Raj Rangaraju, Anil Kumar, Ramesh Kumar, Vikas Patil, H. V. Ramakrishna, Ph.D., Pritha Choudhury, Ph.D., Siuli Sarkar, Ph.D., Paul Salerno, "Low-temperature Solders SMT Process Optimization for Enhanced Reliability", Proceedings of SMTA International, Nov. 15 - Dec. 31, 2021.

[2] Morgana Ribas, Ph.D., Anil Kumar, Divya Kosuri, Raghu R. Rangaraju, Pritha Choudhury, Ph.D., Suresh Telu, Ph.D., Siuli Sarkar, Ph.D., "LOW TEMPERATURE SOLDERING USING SN-BI ALLOYS", Proceedings of SMTA International, Sep. 17 – 21, 2017, Rosemont, IL, USA

[3] Britta Schafsteller, Karl Gerdom, Gustavo Ramos, "Impact of the Surface Finish on IMC and Solder Joint Reliability with Low Temperature Solder Paste", Proceedings of SMTA International, Nov. 15 – Dec. 31, 2021.

[4] Jungsoo Kim, Seung-Boo Jung, Jeong-Won Yoon, "Effect of a phosphorous-containing Pd layer in a thin-ENEPIG surface finish on the interfacial reactions and mechanical strength of a Sn-58Bi solder joint", Journal of Alloys and Compounds, 820 (2020) 153396

[5] Jungsoo Kim, Dae-Young Park, Byeongjin Ahn, Junghwan Bang, Min-Su Kim, Hyun-Soon Park, Yoonchul Sohn, Yong-Ho Ko, "Effective (Pd,Ni)Sn4 diffusion barrier to suppress brittle fracture at Sn-58Bi-xAg solder joint with Ni(P)/Pd(P)/Au metallization pad", Microelectronics Reliability 129 (2022) 114472

[6] S Paiman, Q Gao, H J Joyce, Y Kim, H H Tan, C Jagadish, X Zhang, Y Guo, J Zou, "Growth temperature and V/III ratio effects on the morphology and crystal structure of InP nanowires", Journal of Physics D: Applied Physics, 43 (2010) 445402